

# Overall Formulation for Multilayer SIW Circuits based on Addition Theorems and the Generalized Scattering Matrix

Jesús Rubio, Alfonso Gómez García, Rafael Gómez Alcalá, *Member, IEEE*, Yolanda Campos-Roca, and Juan Zapata, *Senior Member, IEEE*

**Abstract**—This letter presents a multilayer formulation for Substrate Integrated Waveguide circuits, based on the analytical connection of cylindrical modes of sections described by their Generalized Scattering Matrix (GSM). Sections containing arbitrary elements, defined by feeding and cylindrical ports, are analyzed by using the Finite Element Method with fast frequency sweep to obtain their GSM.

**Index Terms**—Substrate Integrated Waveguide (SIW) circuits, Generalized Scattering Matrix, addition theorems, cylindrical modes, Finite Element Method (FEM), fast frequency sweep.

## I. INTRODUCTION

OVER the last few years, Substrate Integrated Waveguide (SIW) technology has attracted the interest of designers of microwave and millimeter-wave circuits due to its low cost, light weight and easy integration. Because of this, a great effort to develop efficient analysis techniques is being made. One of the most efficient techniques consists in calculating the multiple scattering of circular metallic or dielectric posts by using the addition theorems, hybridized with Mode-Matching (MM) [1] or with the Method of Moments (MoM) [2] to feed with rectangular ports, or with the MoM and MM to feed through slots or vertical coax [3]. It has also been extended to stacked geometries [4].

In this work, we introduce an overall formulation based on the Generalized Scattering Matrix (GSM) and the addition theorems for cylindrical modes, capable of coupling the feeding through a few cylindrical modes, keeping the size of the final system equal to the total number of cylindrical modes. The use of the Finite Element Method (FEM) to obtain the GSM allows us to analyze more complicated feeders, and arbitrary resonators, posts or slots. Additionally, local rotations for sections without rotational symmetry are included analytically, which can be useful for design. Finally, the efficiency of the FEM is increased by extending the fast frequency sweep method given in [5] to cylindrical ports.

## II. OVERALL FORMULATION

Consider the multilayer SIW circuit given by Fig. 1. In this circuit we can identify sections bounded individually, in the

Manuscript received January 10, 2018; revised February 27; accepted April 20. This work was supported by MINECO/AEI/FEDER, UE, Spain, under projects TEC2017-83352-C2-2-P and TEC2017-83352-C2-1-P.

J. Zapata is with E.T.S.I.Telecomunicación, Avda. de la Complutense, Universidad Politécnica de Madrid, 28040 Madrid, Spain. The rest of the authors are with Escuela Politécnica, Universidad de Extremadura, Avda. de la Universidad, s/n 10003 Cáceres, Spain. (E-mail: jesusrubio@unex.es)

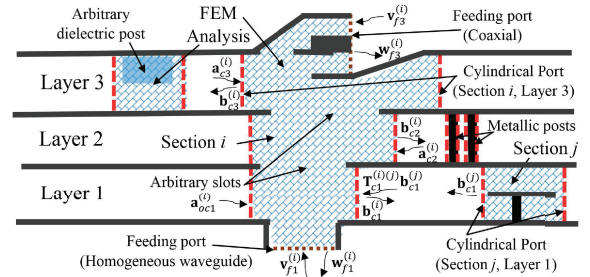


Fig. 1. Side view of a multilayer microwave circuit.

most general case, by a cylindrical port and a feeding port for each layer. These sections contain any kind of discontinuity between the parallel plates and their cylindrical ports cannot overlap with each other. Each section  $i$  can be described by their GSM given by

$$\begin{bmatrix} \mathbf{S}_{f1,f1}^{(i)} \dots \mathbf{S}_{f1,fK}^{(i)} \mathbf{S}_{f1,c1}^{(i)} \dots \mathbf{S}_{f1,cK}^{(i)} \\ \vdots \\ \mathbf{S}_{fK,f1}^{(i)} \dots \mathbf{S}_{fK,fK}^{(i)} \mathbf{S}_{fK,c1}^{(i)} \dots \mathbf{S}_{fK,cK}^{(i)} \\ \mathbf{S}_{c1,f1}^{(i)} \dots \mathbf{S}_{c1,fK}^{(i)} \mathbf{S}_{c1,c1}^{(i)} \dots \mathbf{S}_{c1,cK}^{(i)} \\ \vdots \\ \mathbf{S}_{cK,f1}^{(i)} \dots \mathbf{S}_{cK,fK}^{(i)} \mathbf{S}_{cK,c1}^{(i)} \dots \mathbf{S}_{cK,cK}^{(i)} \end{bmatrix} \begin{bmatrix} \mathbf{v}_{f1}^{(i)} \\ \vdots \\ \mathbf{v}_{fK}^{(i)} \\ \mathbf{a}_{c1}^{(i)} \\ \vdots \\ \mathbf{a}_{cK}^{(i)} \end{bmatrix} = \begin{bmatrix} \mathbf{w}_{f1}^{(i)} \\ \vdots \\ \mathbf{w}_{fK}^{(i)} \\ \mathbf{b}_{c1}^{(i)} \\ \vdots \\ \mathbf{b}_{cK}^{(i)} \end{bmatrix}, \quad (1)$$

where  $\mathbf{v}_{fK}^{(i)}$  and  $\mathbf{w}_{fK}^{(i)}$  are column vectors of complex amplitudes of incident and reflected modes on the feeding ports of section  $i$  in layer  $K$ , and  $\mathbf{a}_{cK}^{(i)}$  and  $\mathbf{b}_{cK}^{(i)}$  are column vectors of complex amplitudes of standing and scattered cylindrical modes on a cylindrical port of section  $i$  in layer  $K$ .

For each layer  $K$ , the incident field on the cylindrical port of section  $i$  is given by the superposition of the field coming from outside the group of cylinders, and the contribution of the field scattered by the other cylinders in this layer referred to the cylindrical port of section  $i$ . These fields can be expressed in terms of complex amplitudes of cylindrical modes

$$\mathbf{a}_{cK}^{(i)} = \mathbf{a}_{ocK}^{(i)} + \sum_{j \neq i, i, j \in \text{layer } K} \mathbf{T}_{cK}^{(i)(j)} \mathbf{b}_{cK}^{(j)}, \quad (2)$$

where  $\mathbf{a}_{ocK}^{(i)}$  accounts for the field coming from outside, and  $\mathbf{T}_{cK}^{(i)(j)}$  is the general translational matrix, whose elements are

$$t_{cK}^{(i)(j)}(m_i, m_j) = e^{j m_i (\varphi(r_i) - \varphi_j)} H_{m_j - m_i}^{(2)}(k_\rho d_{ji}) e^{j m_j (\varphi_{ji} - \varphi(r_j))} \quad (3)$$

with  $H_{m_j-m_i}^{(2)}$  denoting the Hankel function,  $m_i$  and  $m_j$  are the indexes of cylindrical modes related to  $\varphi$ -dependence on cylindrical ports in layer  $K$  for sections  $i$  and  $j$  respectively,  $d_{ji}$  is the distance between these cylinders,  $k_\rho$  is the radial wavenumber [3] of the cylindrical modes,  $\varphi_{ji}$  is the angle defined in a local coordinate system in the cylindrical port of section  $j$  from the axis of this cylindrical port to the axis of the cylindrical port of section  $i$ , and  $\varphi(r_i), \varphi(r_j)$  are the rotation angles defining local rotations of both cylindrical ports. Substituting (2) in (1) for every section and sorting terms layer to layer the following equations can be obtained

$$\begin{bmatrix} \mathbf{S}_{f1,f1} \dots \mathbf{S}_{f1,fK} \\ \vdots \\ \mathbf{S}_{fK,f1} \dots \mathbf{S}_{fK,fK} \end{bmatrix} \begin{bmatrix} \mathbf{v}_{f1} \\ \vdots \\ \mathbf{v}_{fK} \end{bmatrix} + \begin{bmatrix} \mathbf{S}_{f1,c1} \dots \mathbf{S}_{f1,cK} \\ \vdots \\ \mathbf{S}_{fK,c1} \dots \mathbf{S}_{fK,cK} \end{bmatrix} \begin{bmatrix} \mathbf{a}_{oc1} \\ \vdots \\ \mathbf{a}_{ocK} \end{bmatrix} + \begin{bmatrix} \mathbf{S}_{f1,c1} \dots \mathbf{S}_{f1,cK} \\ \vdots \\ \mathbf{S}_{fK,c1} \dots \mathbf{S}_{fK,cK} \end{bmatrix} \begin{bmatrix} \mathbf{T}_{c1} & \mathbf{0} & \mathbf{0} \\ \mathbf{0} & \ddots & \mathbf{0} \\ \mathbf{0} & \mathbf{0} & \mathbf{T}_{cK} \end{bmatrix} \begin{bmatrix} \mathbf{b}_{c1} \\ \vdots \\ \mathbf{b}_{cK} \end{bmatrix} = \begin{bmatrix} \mathbf{w}_{f1} \\ \vdots \\ \mathbf{w}_{fK} \end{bmatrix} \quad (4)$$

$$\begin{bmatrix} \mathbf{S}_{c1,f1} \dots \mathbf{S}_{c1,fK} \\ \vdots \\ \mathbf{S}_{cK,f1} \dots \mathbf{S}_{cK,fK} \end{bmatrix} \begin{bmatrix} \mathbf{v}_{f1} \\ \vdots \\ \mathbf{v}_{fK} \end{bmatrix} + \begin{bmatrix} \mathbf{S}_{c1,c1} \dots \mathbf{S}_{c1,cK} \\ \vdots \\ \mathbf{S}_{cK,c1} \dots \mathbf{S}_{cK,cK} \end{bmatrix} \begin{bmatrix} \mathbf{a}_{oc1} \\ \vdots \\ \mathbf{a}_{ocK} \end{bmatrix} + \begin{bmatrix} \mathbf{S}_{c1,c1} \dots \mathbf{S}_{c1,cK} \\ \vdots \\ \mathbf{S}_{cK,c1} \dots \mathbf{S}_{cK,cK} \end{bmatrix} \begin{bmatrix} \mathbf{T}_{c1} & \mathbf{0} & \mathbf{0} \\ \mathbf{0} & \ddots & \mathbf{0} \\ \mathbf{0} & \mathbf{0} & \mathbf{T}_{cK} \end{bmatrix} \begin{bmatrix} \mathbf{b}_{c1} \\ \vdots \\ \mathbf{b}_{cK} \end{bmatrix} = \begin{bmatrix} \mathbf{b}_{c1} \\ \vdots \\ \mathbf{b}_{cK} \end{bmatrix} \quad (5)$$

where, for each layer  $K$ ,  $\mathbf{v}_{fK}$  and  $\mathbf{w}_{fK}$  are vectors whose dimension is the total number of feeding modes in this layer, since they are formed by subvectors  $\mathbf{v}_{fK}^{(i)}$  and  $\mathbf{w}_{fK}^{(i)}$  respectively, corresponding to all sections with feeding ports in layer  $K$ .  $\mathbf{a}_{ocK}$  and  $\mathbf{b}_{cK}$  are vectors whose dimension is the sum of cylindrical modes in this layer since they are formed by subvectors  $\mathbf{a}_{ocK}^{(i)}$  and  $\mathbf{b}_{cK}^{(i)}$  respectively, corresponding to all the cylindrical ports in layer  $K$ . And  $\mathbf{T}_{cK}$  is a matrix whose submatrices are the general translational matrices  $\mathbf{T}_{cK}^{(i)(j)}$  referred to in (2).

Eqs. (4) and (5) can be expressed in a more compact way

$$\mathbf{S}_{ff} \mathbf{v}_f + \mathbf{S}_{fc} \mathbf{a}_{oc} + \mathbf{S}_{fc} \mathbf{T}_c \mathbf{b}_c = \mathbf{w}_f \quad (6)$$

$$\mathbf{S}_{cf} \mathbf{v}_f + \mathbf{S}_{cc} \mathbf{a}_{oc} + \mathbf{S}_{cc} \mathbf{T}_c \mathbf{b}_c = \mathbf{b}_c. \quad (7)$$

By imposing no field coming from outside the groups of cylinders ( $\mathbf{a}_{oc} = \mathbf{0}$ ), solving the implicit equation (7) to find  $\mathbf{b}_c$  and substituting it in (6), we obtain

$$(\mathbf{S}_{ff} + \mathbf{S}_{fc} \mathbf{T}_c (\mathbf{I} - \mathbf{S}_{cc} \mathbf{T}_c)^{-1} \mathbf{S}_{cf}) \mathbf{v}_f = \mathbf{w}_f, \quad (8)$$

with  $\mathbf{I}$  being the identity matrix. In this way, starting from the GSM of every section and by using the general translational matrices, all reflection and transmission S parameters defined as in [6] between the feeding modes can be directly obtained.

### III. FINITE ELEMENT METHOD WITH FAST FREQUENCY SWEEP FOR CYLINDRICAL PORTS

In order to compute (8), it is necessary to obtain the GSM of each section. If the section consists of a circular metallic or dielectric post, the GSM reduces to an analytical scattering matrix [1]. However, for a more general kind of section,

including the feeder, non circular posts, arbitrary resonators or arbitrarily shaped slots between two layers, a numerical solution could be required. The Finite Element/Modal Analysis method [6] allows us to obtain the GSM from the Generalized Admittance Matrix (GAM), given by

$$\mathbf{Y}(k) = j \frac{k}{\eta_0} \mathbf{B}_N^T(k) [\mathbf{K} - k^2 \mathbf{M}]^{-1} \mathbf{B}_N(k), \quad (9)$$

where  $\mathbf{K}$  and  $\mathbf{M}$  are the standard FEM matrices,  $k$  is the wavenumber,  $\eta_0$  is the intrinsic impedance of vacuum and the elements of matrix  $\mathbf{B}_N(k)$ , for port  $p$  and mode  $j$ , are

$$b_{qj}^p = \int_{S_p} \mathbf{F}_q \cdot (\mathbf{n}_p \times \mathbf{e}_{tj}^{(p)}) dS_p / \int_{S_p} \mathbf{h}_{tj}^{(p)} \cdot (\mathbf{n}_p \times \mathbf{e}_{tj}^{(p)}) dS_p. \quad (10)$$

They account for the coupling between  $\mathbf{F}_q$  (Interpolation Functions of FEM) and the tangential electric field  $\mathbf{e}_{tj}$  on the surface port  $S_p$ . In (10),  $\mathbf{h}_{tj}$  is the tangential magnetic field and  $\mathbf{n}_p$  is a normal vector to  $S_p$ . This multimode FEM formulation is suitable for a reliable fast frequency sweep when we can achieve the following factorization where  $k_0$  can be any wavenumber of analysis [5]

$$\mathbf{B}_N(k) = \mathbf{B}_N(k_0) \mathbf{J}(k, k_0), \quad (11)$$

as is the case of TEM, TE and TM modes of uniform waveguides [6]. In the case of  $\text{TE}^z$  cylindrical modes this factorization is feasible and the elements of  $\mathbf{J}$  are given by

$$J_j(k, k_0) = (1 - k_{cj}^2/k_0^2)^{1/4} / (1 - k_{cj}^2/k^2)^{1/4}, \quad (12)$$

with  $k_{cj}$  being the cutoff wavenumber of each mode  $j$ . However, a factorization is not possible for  $\text{TM}^z$  cylindrical modes since  $e_\varphi$  and  $e_z$  components of the tangential electric field do not share the same frequency dependence.

In order to overcome this problem, we have decomposed (10), taking advantage of the  $\text{TM}^z$  definition ( $h_z = 0$ )

$$b_{qj}^{(p)} = \left( \int_{S_p} \mathbf{F}_q \cdot (\mathbf{n}_p \times e_{zj}^{(p)} \hat{z}) dS_p / \int_{S_p} h_{\varphi j}^{(p)} e_{zj}^{(p)} dS_p \right) + \left( \int_{S_p} \mathbf{F}_q \cdot (\mathbf{n}_p \times e_{\varphi j}^{(p)} \hat{\varphi}) dS_p / \int_{S_p} h_{\varphi j}^{(p)} e_{zj}^{(p)} dS_p \right), \quad (13)$$

which makes it possible to decompose each column of  $\mathbf{B}_N(k)$  corresponding to each  $\text{TM}^z$  mode in two columns. Each of these two columns can be factored as (11), with

$$J_{zj}(k, k_0) = (1 - k_{cj}^2/k^2)^{1/4} / (1 - k_{cj}^2/k_0^2)^{(1/4)} \quad (14)$$

$$J_{\varphi j}(k, k_0) = (k_0/k)^2 (1 - k_{cj}^2/k_0^2)^{3/4} / (1 - k_{cj}^2/k^2)^{3/4}. \quad (15)$$

Now, the frequency sweep can be efficiently carried out to obtain a pseudo-GAM [6]. This pseudo-GAM is subsequently corrected by using  $\mathbf{J}$ . Finally, the GAM is obtained by merging the two columns and the two rows corresponding to the two terms in which each  $\text{TM}^z$  mode was decomposed.

### IV. VALIDATION AND RESULTS

Next, three application examples are shown. In all of them, metallic posts requires 5 modes. Other sections have been analyzed with FEM and fast frequency sweep. The number of cylindrical modes has been chosen according to [1]. Other

sections have been analyzed with FEM and fast frequency sweep. In the worst case, the CPU time required to perform the fast frequency sweep has been equivalent to that needed to obtain seven frequency points. Our results have been validated with CST [7]. Table I shows speedups up to 59 times w.r.t. CST.

The first example is a SIW resonator. This device has a via hole rounded by a circular slot connected to the top through a metallic contact placed at the angle  $\phi$  for tuning purposes [8]. The GSM of this element is described by 7 cylindrical modes with just one FEM simulation, since the angle  $\phi$  is introduced analytically. Fig. 2 shows a comparison between the results obtained and the measurements in [8] for an empty cavity, and for  $\phi$  equal to  $0^\circ$  and  $180^\circ$ . Deviations in  $S_{21}$  are attributed to the fact that all of our simulations are lossless.

The second example is the coaxial to SIW transition designed in [9], analyzed using a cylindrical port surrounding it, as shown in Fig. 3. Its GSM is defined in terms of the TEM coaxial mode and 35 cylindrical modes, hardly increasing the computational cost of evaluating (8) when used in a SIW circuit. Fig. 3 also displays the results of using a SIW section to interconnect two faced transition elements, being one rotated  $180^\circ$ .

The last example, shown in Fig. 4, is a multilayer power divider based on two coupling slots [10]. Each slot is described with only 13 cylindrical modes for a top-layer cylinder over the slot, and an equal number of modes for its down-layer counterpart. SIW ports are included with a FEM simulation of a transition between an equivalent rectangular waveguide and a cylindrical port with 19 modes. This kind of designs can be carried out very fast by precomputed simulations of slots of different size. They can be used as a lookup table in a design process, where in each analysis cycle only (8) is required to be computed.

TABLE I

SIMUL. TIME PER FREQ. (XEON E5-2620 2.4 GHZ 64 GB RAM)

GSM of FEM sections			Computation of (8)			Speedup w.r.t. CST		
Fig.2	Fig.3	Fig.4	Fig.2	Fig.3	Fig.4	Fig.2	Fig.3	Fig.4
0.64s	10.2s	12.4s	0.02s	0.02s	0.6s	x10	x59	x20

## V. CONCLUSION

A multilayer formulation for SIW circuits, which includes the feeding through a few cylindrical modes, has been presented. It is based on the GSM and additions theorems for cylinders. It has also been shown that a fast frequency sweep to compute the GSM of arbitrary sections with cylindrical ports, by means of the FEM, can be applied. Design of SIW devices can be performed very fast, since rotations and positions of each element are introduced analytically. GSMs of different elements can also be used based on previous FEM simulations, and stored in a lookup table for the optimization process.

## REFERENCES

- [1] E. Diaz-Caballero, H. Esteban, A. Belenguier and V. Boria, "Efficient analysis of substrate integrated waveguide devices using hybrid mode matching between cylindrical and guided modes", *IEEE Trans. Microw. Theory Techn.*, vol. 60, no. 2, pp. 232-243, Feb. 2012.
- [2] X. Wu and A. Kishk, "Hybrid of method of moments and cylindrical eigenfunction expansion to study substrate integrated waveguide circuits," *IEEE Trans. Microw. Theory Techn.*, vol. 56, no. 10, pp. 2270-2276, Oct. 2008.

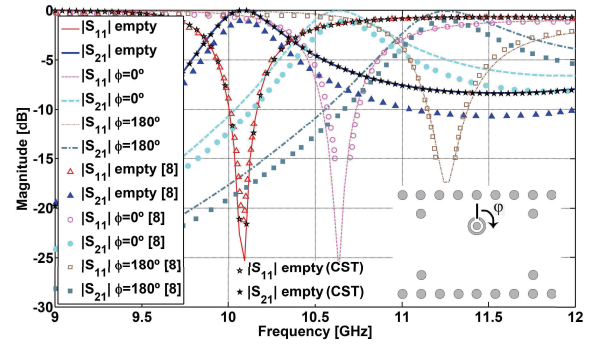


Fig. 2. SIW resonator (top view) and its scattering parameters compared with measurements [8].

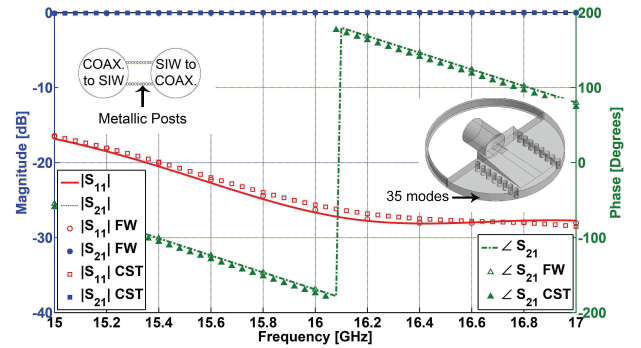


Fig. 3. Configuration and results for a SIW section connected by lateral coax to SIW transitions, compared with a full-wave FEM (FW) [6] and CST.

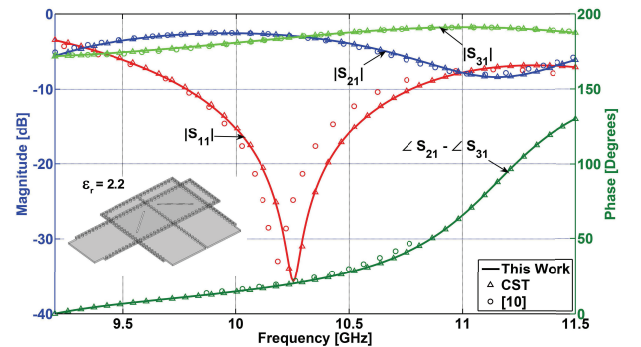


Fig. 4. Scattering parameters for the multilayer power divider from [10].

- [3] M. Casaletti, R. Sauleau, M. Ettore, and S. Maci, "Efficient analysis of metallic and dielectric posts in parallel-plate waveguide structures," *IEEE Trans. Microw. Theory Techn.*, vol. 60, no. 10, pp. 2979-2989, Oct. 2012.
- [4] M. Casaletti, G. Valerio, J. Seljan, M. Ettore, and R. Sauleau, "A full-wave hybrid method for the analysis of multilayered SIW-based antennas," *IEEE Trans. Antennas Propag.*, vol. 61, no. 11, pp. 5575-5588, Nov. 2013.
- [5] V. de la Rubia, U. Razafison, and Y. Maday, "Reliable fast frequency sweep for microwave devices via the reduced-basis method," *IEEE Trans. Microw. Theory Techn.*, vol. 57, no. 12, pp. 2923-2937, Dec. 2009.
- [6] J. Rubio, J. Arroyo, and J. Zapata, "SFELP-An efficient methodology for microwave circuit analysis," *IEEE Trans. Microw. Theory Techn.*, vol. 49, no. 3, pp. 509-516, Mar. 2001.
- [7] 3D EM Field Simulation CST. Available: <http://www.cst.com>.
- [8] F. Mira, J. Mateu, and C. Collado, "Mechanical tuning of substrate integrated waveguide resonators", *IEEE Microw. Compon. Lett.*, vol. 22, no. 9, pp. 447-449, Sept. 2012.
- [9] P. Chen, W. Hong, Z. Kuai, J. Xu, H. Wang, J. Chen, H. Tang, J. Zhou, and K. Wu, "A multibeam antenna based on substrate integrated waveguide technology for MIMO wireless communications", *IEEE Trans. Antennas Propag.*, vol. 57, no. 6, pp. 1813-1821, Jun. 2009.
- [10] R. Tiwari, S. Mukherjee, and A. Biswas, "Design and characterization of multi-layer Substrate Integrated Waveguide (SIW) slot coupler". In *European Conf. Antennas and Propagation (EuCAP)*, pp. 1-4, 2015.